IAES International Journal of Artificial Intelligence (IJ-AI)
Vol. 13, No. 4, December 2024, pp. 4939~4947
ISSN: 2252-8938, DOI: 10.11591/ijai.v13.i4.pp4939-4947

Enhancing ultrasound-guided brachial plexus nerve localization with ResNet50 and support vector machine

Sobhana Mummaneni, Kushal Kumar Chintakayala, Lalith Sai Mukund Yarlagadda, Venkata Siva Naga Raju Ala, Nihitha Vemulapalli
Department of Computer Science and Engineering, Velagapudi Ramakrishna Siddhartha Engineering College, Vijayawada, India

Article Info

Article history:

Received Dec 15, 2023
Revised Mar 1, 2024
Accepted Mar 21, 2024

Keywords:

Brachial plexus
Peripheral nerve blocking
ResNet50
Segmentation
Support vector machine classifier

ABSTRACT

Medical image segmentation and classification plays a vital role in nerve block/region identification, particularly for anesthesiologists relying on instinctual judgments. However, due to patient-specific anatomical variations, these methods sometimes lack precision. This research focuses on addressing the problem, by incorporating novel ensembling method of ResNet-50 and support vector machine (SVM) to achieve segmentation of dataset images and classification of nerve blocks respectively. The said novel ensemble model is trained on a publicly available dataset consisting of more than 16,800 images. The sole purpose of this work is to address the problem of peripheral nerve blocking (PNB) with the usage of ensemble modelling, while achieving the highest possible accuracy. This research will help practitioners in accurately identifying the location of brachial plexus and distinguishing the type of nerve block to be injected – interscalene and supraclavicular. The model, which integrates ResNet50 and SVM classifier, achieved a commendable 99.27% accuracy in identifying and classifying the brachial plexus region.

Corresponding Author:

Sobhana Mummaneni
Department of Computer Science and Engineering, Velagapudi Ramakrishna Siddhartha Engineering College
Vijayawada 520007, India
Email: sobhana@vrsiddhartha.ac.in

1. INTRODUCTION

Anesthesiologists have always intuitively recognized nerve blocks and regions through the segmentation of medical images [1]. When it comes to precisely where to deliver anesthesia, they typically rely on their intuition and experience. However, because each patient's area of administration has unique dynamics, this process may not always produce 100% accuracy. As a result, blood pressure (BP) nerves can be found on ultrasonography pictures that identify nerve structures. Identification can be difficult even for specialists in the field since speckle noise and echo disruptions [2] can cause the ultrasound pictures to become distorted. By using pain management catheters, this treatment acts as a help and facilitates practitioners' ability to operate on nerves efficiently, which eases processes like peripheral nerve blockage (PNB) and regional anesthetic [3], [4].

There have been several works that focused on the detection of brachial plexus region [5] in the inputted ultrasound images; but this approach involves detection as well as segmentation of the brachial plexus region, into supraclavicular and interscalene [6], and this work would be the first of its kind. The concepts of supraclavicular and interscalene nerve blocks are medically complex, and a practitioner needs to be able to thoroughly differentiate between them. An interscalene nerve block is injected between the muscles of the neck region, which is in between the scalene muscles. This nerve block specifically affects the nerves that extend to the shoulders and the upper arm and provides effective anesthesia for operations performed on the same. On the contrary, a supraclavicular is injected above the collarbone, in the region just above the shoulder, and it affects the brachial plexus nerves in a similar manner, except for the fact that it provides anesthesia for the entire arm, and hence is used for operations that involve hand, forearm and elbow regions.

Residual network with 50 layers (ResNet50) and support vector machine (SVM) hybrid model combines the strengths of convolutional neural networks (CNNs) and traditional machine learning algorithms to create a powerful classification system. ResNet50, a variant of the deep residual network architecture, serves as the feature extractor, leveraging its ability to capture complex hierarchical patterns in images. The pretrained ResNet50 model is utilized to extract high-level features [7] from input images, preserving spatial relationships and semantic information. These extracted features are then fed into a SVM classifier, which excels in handling high-dimensional feature spaces and finding optimal decision boundaries.

The decision of choosing between the right nerve block depends on the complexity of surgical procedure and the considerations of the anesthesia provider. Anesthesiologists carefully assess the patient's medical history, current health status, and the nature of the surgical procedure to determine the appropriate type and amount of anesthesia. Practitioner's tailor the dosage to each patient's specific requirements, ensuring optimal anesthetic effects and minimizing risks. In the event of unexpected complications or emergencies during surgery, they must be prepared to respond quickly and adjust the anesthesia dosage to address the situation while maintaining patient safety.

The paper is organized into five sections. The first section shows the introduction part. The second section is literature review, focused on existing research related to our study. The third section is methodology, which details our approach and techniques applied. The fourth section is results and discussion, which presents our findings. Finally, the conclusion section summarizes the findings and future work.

2. LITERATURE REVIEW

Kaye *et al.* [8] clearly and concisely delineated the distinctions between supraclavicular and interscalene nerve blocks. They presented evidence from several studies indicating that, from a safety standpoint, interscalene blocks are often preferred. However, both interscalene and supraclavicular blocks are endorsed as highly safe methods for administering regional anesthesia, particularly when applied with ultrasound guidance. This assessment underscores the importance of choosing the appropriate nerve block technique based on safety, efficacy, and the specific clinical context, highlighting the advancements in ultrasound-guided regional anesthesia practices.

Gao *et al.* [9] conducted a survey on UTNet, a hybrid transformer for medical image segmentation, which combines convolutional networks with self-attention modules. It demonstrates superior performance and robustness, showing promise for medical vision, although this field remains largely unexplored. Dhabhai and Gupta [10] examined medical data growth, emphasizing SVM's efficiency in image classification. Their review highlights SVM's accuracy and effectiveness for managing expanding medical image datasets.

Maruyama *et al.* [11] compared medical image classification accuracy across SVM, artificial neural network (ANN), and CNN models. They investigated the impact of low-quality images on accuracy using JPEG and DICOM datasets, finding CNN to outperform others in efficiency and accuracy. Cai *et al.* [12] analyzed big medical data's role in medical imaging with deep learning, highlighting its success in image detection, segmentation, and classification. They discussed challenges, 5G's impact, and predicted intelligent medical device advancements.

Zhou *et al.* [13] introduced a novel active contour model for medical image segmentation, utilizing a unified Gaussian distribution framework. It combines global and local energy terms to enhance contour evolution and precision. Adaptive weighting improves handling of intensity inhomogeneities, showing superior efficiency and accuracy in extensive synthetic and real image tests. Shah *et al.* [14] explored rice disease detection using deep learning and transfer learning with models like ResNet50, achieving up to 99.75% accuracy. This research serves as a reference for understanding the performance of Inception V3, VGG 16, CNN, and ResNet50 frameworks for classic detection problems.

Ikechukwu *et al.* [15] compared ResNet-50, VGG-19, and traditional training for classifying pneumonia from chest x-rays. Highlighting deep learning's high computational demands, they noted dropout regularization's role in efficiency. Their approach achieved a 92.03% recall, matching fine-tuned pre-trained models. Khairandish *et al.* [16] explored magnetic resonance imaging (MRI) brain image classification and tumor detection using a CNN-SVM hybrid. Achieving 98.4959% accuracy, this methodology demonstrates the hybrid's effectiveness, utilizing statistical functions and the BRATS 2015 dataset, derived from earlier versions, for comprehensive analysis and significant tumor detection advancements.

Ding *et al.* [17] segmented the brachial plexus in ultrasound images using MallesNet, based on R-CNN and enhanced with short-lived climate forcers (SLCF) and stochastic average gradient (SAG) for detailed contrast and spatial features. A local dataset of 101 patient images validated the method's effectiveness. Bowness *et al.* [18] compared anesthesiologist assessments and AI-generated color overlays by ScanNav on ultrasound images for ultrasound-guided regional anaesthesia (UGRA). Utilizing dice and Hausdorff coefficients, they analyzed various nerve blocks, finding both human and AI approaches highly accurate, with humans showing consistent scores and AI exhibiting minimal variation.

Jo *et al.* [19] explored supraclavicular block segmentation using computer-aided diagnosis (CADx) and CNNs, contrasting traditional image datasets with video data for enhanced Standard Chartered Bank (SCB) administration. They integrated ResNet for classification and U-Net for segmentation within a cascading framework, offering an in-depth comparative analysis of various CNN models, enhancing detection and segmentation accuracy. Tian *et al.* [20] evaluated 12 deep learning models for brachial plexus segmentation in ultrasound images, critical for anesthesia. U-Net excelled with 68.50% intersection over union (IoU) but slow processing, whereas LinkNet balanced speed and accuracy, ideal for real-time use. Challenges include a small dataset and the need for future advancements.

3. METHODOLOGY

The following system architecture in Figure 1 clearly portrays the working methodology and required parameters. For a better understanding. The phases in the suggested model are shown in this process flow diagram. Following are the main modules of the flow diagram: ultrasound image dataset, data preprocessing module, model training, model evaluation, and regional classification. Each module has its own usage, to produce the final masked image of the ultrasound images. Incorporating separate models for segmentation and classification helps in achieving results with higher accuracy. SVM algorithms are widely known for their excellent performance in image classification.

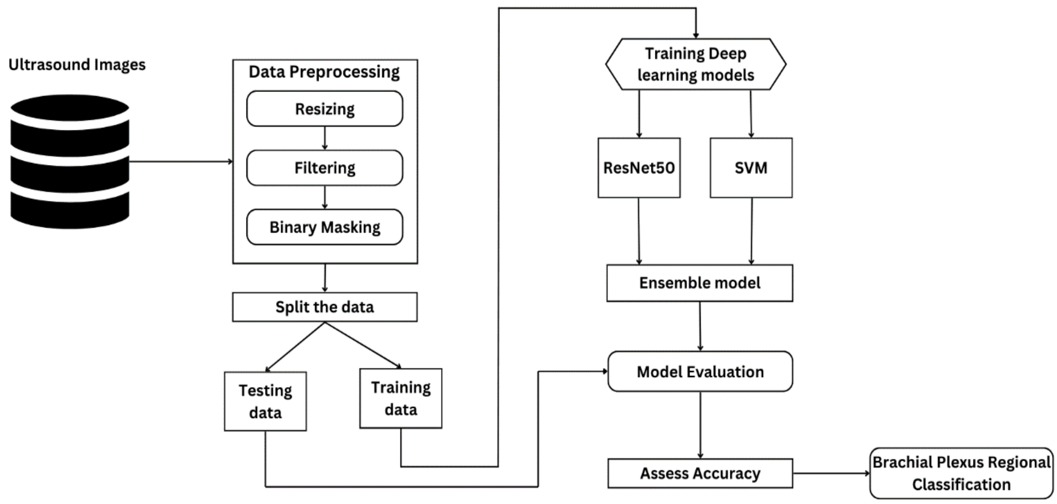

Figure 1. Process flow diagram of the proposed segmentation and classification model

3.1. Ultrasound image dataset

A dataset has been used, which is available on Kaggle [21], for an extensive dataset is needed to train both ResNet and SVM models. This dataset consists of raw images of brachial plexus that were manually annotated by humans. It is noteworthy that individuals who annotated these images are trained professionals and are asked to annotate the images where they are confident of identifying the presence of brachial plexus. Given that it is all human annotated data, there will undeniably be presence of Noise, Artifacts, and even potential mistakes. Elimination of these irregularities needs to be carried out so that they won't hinder the result.

3.2. Data preprocessing

Data preprocessing [22] in image segmentation denotes the set of techniques applied on raw image data, before being given as an input to a machine learning model for segmentation tasks. Image segmentation involves dividing an image into meaningful and distinct regions or objects. To improve the segmentation model's performance and the quality of the input data, effective data preprocessing is essential. Some of the common data preprocessing techniques with respect to image segmentation and classification are image resizing, normalization, noise reduction and mask generation. Several preprocessing techniques have been imposed on the input raw images, which are described as follows.

3.2.1. Image resizing

Image resizing [23], as a preprocessing technique, provides uniformity, computational efficiency, model compatibility, generalization, overfitting prevention, reduced training time, data augmentation. Image resizing is a fundamental preprocessing step that addresses issues related to data consistency, computational efficiency, and model compatibility. It plays a crucial role in preparing image data for various machine learning tasks, including image segmentation, by creating a standardized input format for the model.

3.2.2. Data normalization

Data normalization [24] is a preprocessing technique used to scale and transform input data to a standard range, making it easier for machine learning models to learn patterns and generalize well to new, unseen data. Normalization process typically involves adjusting the scale and distribution of the data without changing its inherent structure. The key aspects include consistent scaling, convergence speed, mitigating sensitivity and saturation avoidance. This is a crucial preprocessing step in image segmentation and classification activities and ensures that the input data is in a suitable form for the machine learning algorithm.

3.2.3. Gaussian filtering

Gaussian filtering [25] is an image filtering technique that involves convolving an image with a Gaussian function, which in turn, is a mathematical function that represents a normal distribution, often used in image processing for its smoothing properties. This process involves sliding the Gaussian Kernel over the image and computing a weighted average of the pixel values within the kernel's neighborhood. Gaussian filter is a bell-shaped curve that assigns weights to the central pixels while gradually decreasing weights as you move away from the center. Key aspects of Gaussian filtering include smoothing, edge detection and feature extraction.

3.2.4. Binary masking

Binary masking [26] is a preprocessing technique commonly used in image segmentation and classification tasks. It involves creating a binary image, also known as a mask, that highlights or isolates specific regions or objects of interest within the original image. It typically contains values of 0 and 1, where 0 represents the regions not of interest, and 1 represents the regions of interest. Binary masking is used for several tasks such as region of interest (ROI) extraction, foreground-background separation and training data modification. Figure 2 illustrates the resultant preprocessed image for an exemplar ultrasound image.

Figure 2. Ultrasound image before and after preprocessing

3.3. Splitting the data

Data splitting, or dividing the data into training and testing sets, is an important stage in machine learning that allows you to assess a model's performance. Data splitting is performed to evaluate how well the model generalizes to new, unobserved data. With respect to the proposed approach, the dataset has been split into a ratio of 80:20.

3.4. Residual network with 50 layers

ResNet-50 [27], often referred to as residual network with 50 layers, is a deep CNN architecture that has shown impressive performance segmentation, object recognition, and photo classification. ResNet-50 belongs to a family of ResNet architectures introduced to provide ways of training deep neural networks. ResNet 50 is used for segmentation, because it consists of skip connections, used to facilitate deep learning networks which mitigate the most common vanishing gradient problem. Algorithm 1 describes the working process of ResNet50 for image classification.

Algorithm 1: ResNet50 algorithm
Input: Input image X, Residual block functions F_i for i = 1, 2, n, Learningrate α
Output: Classification result
1. Initialize the convolutional and batch normalization parameters
2. for i = 1 to n do
3. Forward pass through the residual block:
4. $y = F_i(X)$
5. Update X = y
6. end for
7. Global average pooling: X = GlobalAvgPool(X)
8. Fully connected layer: y = FC(X)
9. Softmax activation: y = Softmax(y)
10. Return y

3.5. Support vector machine classifier

The aim of SVM [28] is to find a hyperplane which separates different classes in the feature space. Ultrasound imaging of the brachial plexus is a medical imaging modality used to visualize nerves in the shoulder region. SVM classifier can be employed for the classification of input images to differentiate between different structures or conditions. It is advantageous for classifying the brachial plexus in ultrasound images by learning and recognizing patterns in the extracted features, ultimately assisting healthcare professionals in making accurate diagnoses. Algorithm 2 describes the working process of SVM for image classification.

Algorithm 2: Image classification using svm
Input: Training data (X_i, y_i), Kernel function K, Regularization parameter C, Unlabeled image X_{test}
Output: Predicted class label for X_{test}
1. Preprocess the data: Feature extraction, and normalization
2. Initialize the parameters: w = 0, b = 0
3. Choose a kernel function K
4. Construct the kernel matrix H using K: $H_{ij} = y_i y_j K(X_i, X_j)$
5. Initialize Lagrange multipliers $\alpha_i = 0$ for i = 1, 2, . . . , N
6. for t = 1 to N_{iter} do
7. Compute the SVM decision function: $f(X) = \sum^{N}_{i=1} \alpha_i y_i K(X_i, X_j) + b$
8. Compute the hinge loss: $L = {}^1/_2 \|w\|^2 + C \sum^{N}_{i=1} \max(0, 1 - y_i f(X_i))$
9. Compute the gradients of L with respect to w and b
10. Update the parameters using gradient descent
11. Project α onto the feasible set
12. end for
13. Classify the test image:
14. Compute the decision function for X_{test}: $f(X_{test}) = \sum^{N}_{i=1} \alpha_i y_i K(X_{test}, X_i) + b$
15. Predicted class label: $y_{pred} = \text{sign}(f(X_{test}))$
16. Return y_{pred}

3.6. Ensemble model

Ensembling ResNet50 with a SVM [29] can create a robust and effective model for various machine learning tasks. ResNet50 excels at feature extraction from complex data, particularly in image recognition tasks. By combining its deep learning capabilities with an SVM classifier, the ensemble model leverages the strengths of both models. ResNet50 extracts intricate hierarchical features, and SVM refines the decision boundaries based on these features, resulting in a more accurate model. This approach leads to an improved performance, as the ensemble benefits from the complementary strengths of deep learning and traditional machine learning techniques.

4. RESULTS AND DISCUSSION

The following section depicts the performance of the proposed ResNet50+SVM ensemble model in classifying the input ultrasound images. While previous works addressed the usage of pre-trained models in achieving the same, none of the works emphasized the usage of ensemble approaches, which proved themselves to be more efficient than traditional models, especially in classification problems. The results mentioned earlier can be displayed as tables, graphs, or figures. The research discussion is made into several sub-sections, namely confusion matrix, receiver-operating characteristic curve (ROC)-area under the curve (AUC), accuracy curve, loss curve, and user interface.

4.1. Confusion matrix and ROC-AUC curve

In the following confusion matrix in Figure 3, a lower number of false positives indicates that the model is making fewer mistakes in predicting positive instances when they are not actually positive. Similarly, a lesser number of false negatives indicates that that the model is making fewer mistakes in failing to identify positive instances. Figure 4 illustrates the ROC-AUC curve with a high value of true positive rate (TPR). When the TPR, also known as sensitivity, approaches 0.99, it indicates that the model is performing exceptionally well in correctly identifying positive instances.

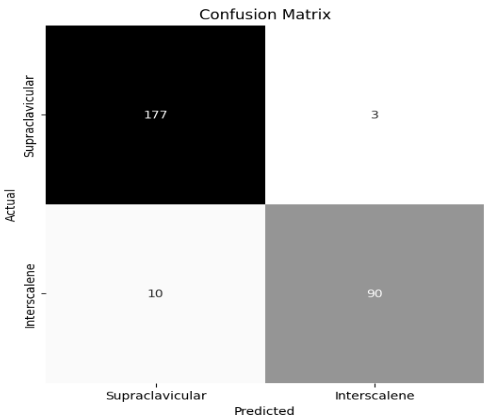

Figure 3. Confusion matrix of ensemble model

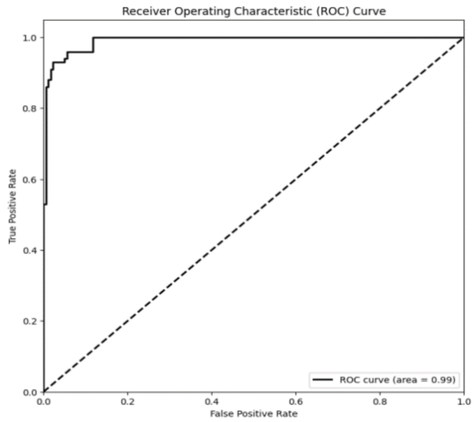

Figure 4. ROC-AUC curve of ensemble model

4.2. Accuracy curve and loss curve

The following Figure 5 clearly indicates that the ensemble model's accuracy is reaching near-100 scores (99.27). In an ensemble model, the training data influences the model's learning process, and this learned knowledge is then applied to make predictions on the testing data. Cross-entropy loss function is illustrated in Figure 6. Training loss measures how well the model fits training data, while testing loss measures how efficiently the model will generalize new and unrevealed data, and hence testing loss needs to be evaluated on a separated dataset.

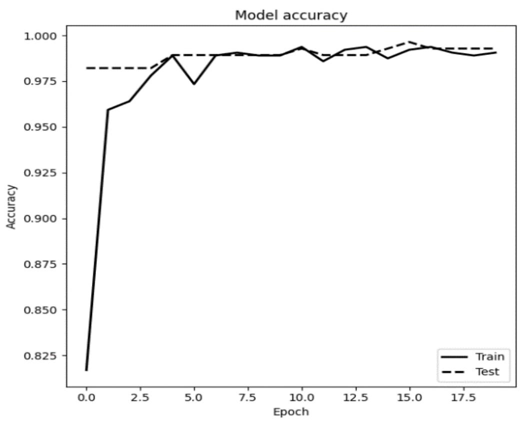

Figure 5. Accuracy curve of the ensemble model

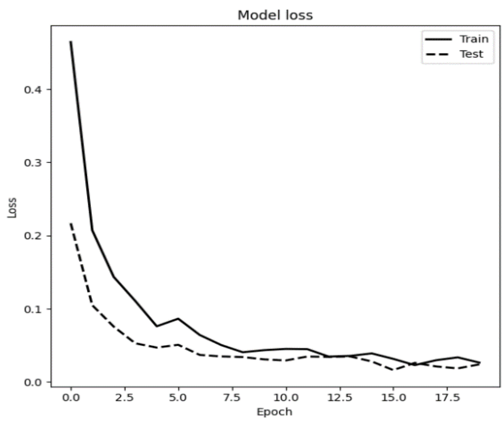

Figure 6. Cross entropy loss function of the ensemble model

4.3. User interface

The result of classification is to be shown using a graphical user interface (GUI). The following figures depict the GUI “image classification App”, which takes a raw user-selected ultrasound image as an input. The output, which is a binary mask, is represented in the same GUI. Figures 7 and 8 depict the classes under which the preprocessed images are classified, namely interscalene and supraclavicular.

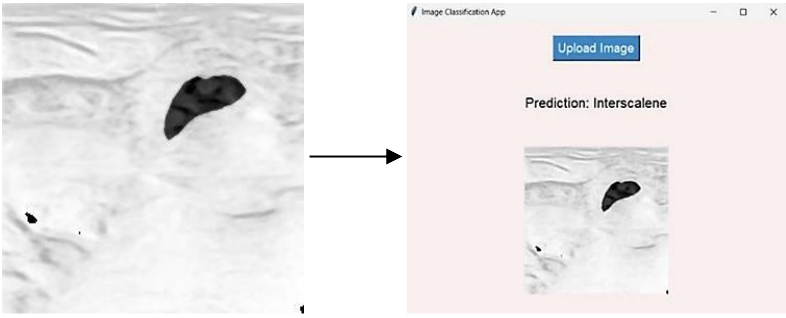

Interscalene

Figure 7. Image classified as interscalene

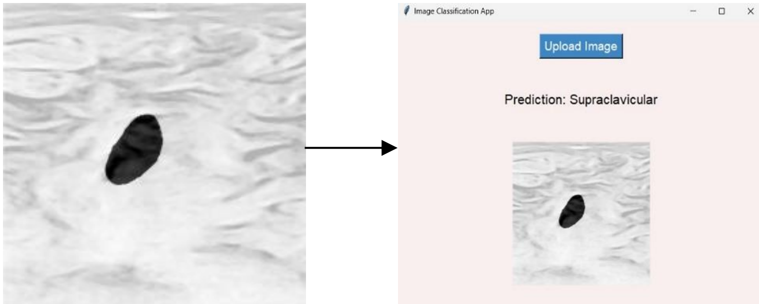

Supraclavicular

Figure 8. Image classified as supraclavicular

5. CONCLUSION

In summary, the primary objective of this work was to develop a highly accurate model for predicting the presence of the brachial plexus nerve region in limbs and classifying it into "interscalene" and "supraclavicular" nerve blocks. This classification is essential, since it helps anesthesiologists determine the type of nerve block, they need to inject, for a particular patient. Although results for previously proposed approaches were promising, brachial plexus anatomy can vary significantly among individuals, including variations in branching patterns and positional relationships with surrounding structures. In addition, extracting relevant features from ultrasound images to represent the anatomical structures of the brachial plexus accurately can be challenging, since it is essential for classification accuracy. Owing to these challenges, employing Resnet50 along with an SVM classifier aims at providing precise outputs which are to be used as an aid by practitioners. While the current focus is on the brachial plexus and ultrasound image inputs, the trained model will be adapted and expanded to encompass various other anatomical regions with appropriate modifications to the algorithms and diverse image datasets through data augmentation. This work sets the foundation for broader applications and collaborations with similar projects, laying the groundwork for advancements in medical image analysis. Looking ahead, there are several promising avenues for future research and development.

REFERENCES

[1] M. H. Hesamian, W. Jia, X. He, and P. Kennedy, “Deep learning techniques for medical image segmentation: achievements and challenges,” *Journal of Digital Imaging*, vol. 32, no. 4, pp. 582-596, Aug. 2019, doi: 10.1007/s10278-019-00227-x.

[2] Y. Eliezer *et al.*, “Suppressing meta-holographic artifacts by laser coherence tuning,” *Light-Science and Applications*, vol. 10, no. 1, May 2021, doi: 10.1038/s41377-021-00547-0.

[3] G. C. Feigl, R. J. Litz, and P. Marhofer, “Anatomy of the brachial plexus and its implications for daily clinical practice: regional anesthesia is applied anatomy,” *Regional Anesthesia and Pain Medicine*, vol. 45, no. 8, pp. 620-627, 2020, doi: 10.1136/rapm-2020-101435.

[4] G. M. Hamilton *et al.*, “Peripheral nerve blocks for ambulatory shoulder surgery: A population-based cohort study of outcomes and resource utilization,” Anesthesiology, vol. 131, no. 6, pp. 1254-1263, Dec. 2019, doi: 10.1097/ALN.0000000000002865.

[5] M. Sobhana, L. S. M. Yarlagadda, K. K. Chintakayala, and V. S. N. R. Ala, "Brachial Plexus segmentation and detection through ultrasound image analysis using convolutional neural networks," *2023 4th IEEE Global Conference for Advancement in Technology (GCAT)*, Bangalore, India, 2023, pp. 1-6, doi: 10.1109/GCAT59970.2023.10353418.

[6] H. Zhang, Z. Qu, Y. Miao, R. Jia, F. Li, and Z. Hua, "Comparison between subparaneural upper trunk and conventional interscalene blocks for arthroscopic shoulder surgery: a randomized noninferiority trial," *Anesthesia and Analgesia,* vol. 134, no. 6, pp. 1308-1317, 2022, doi: 10.1213/ANE.0000000000005990.

[7] M. Suhaidi, R. A. Kadir, and S. Tiun, "A review of feature extraction methods on machine learning," *Journal of Information System and Technology Management*, vol. 6, no. 22, pp. 51–59, Sep. 2021, doi: 10.35631/jistm.622005.

[8] D. Kaye *et al.,* "Supraclavicular vs. infraclavicular brachial plexus nerve blocks: clinical, pharmacological, and anatomical considerations," *Anesthesiology and Pain Medicine*, vol. 11, no. 5, doi: 10.5812/aapm.120658.

[9] Y. Gao, M. Zhou, and D. N. Metaxas, "UTNet: A hybrid transformer architecture for medical image segmentation," in *Medical Image Computing and Computer Assisted Intervention – MICCAI 2021*, Springer, Cham, doi: 10.1007/978-3-030-87199-4_6.

[10] Dhabhai and Y. Gupta, "Empirical study of image classification techniques to classify the image using SVM: A review," *International Journal of Innovative Research in Computer and Communication Engineering*, vol. 4, no. 10, pp. 17128-17133, 2016, doi:10.15680/IJIRCCE.2016.0410004.

[11] T. Maruyama *et al*., "Comparison of medical image classification accuracy among three machine learning methods," *Journal of X-ray Science and Technology*, vol. 26, no. 6, pp. 885-893, 2018, doi: 10.3233/XST-18386.

[12] L. Cai, J. Gao, and D. Zhao, "A review of the application of deep learning in medical image classification and segmentation," *Annals of Translation Medicine*, vol. 8, no. 11, Jun. 2020, doi: 10.21037/atm.2020.02.44.

[13] S. Zhou, J. Wang, S. Zhang, Y. Liang, and Y. Gong, "Active contour model based on local and global intensity information for medical image segmentation," *Neurocomputing*, vol. 186, pp. 107-118, 2016, doi: 10.1016/j.neucom.2015.12.073.

[14] S. R. Shah, S. Qadri, H. Bibi, S. M. W. Shah, M. I. Sharif, and F. Marinello, "Comparing inception V3, VGG 16, VGG 19, CNN, and ResNet 50: A case study on early detection of a rice disease," *Agronomy*, vol. 13, no. 6, 2023, doi: 10.3390/agronomy13061633.

[15] V. Ikechukwu, S. Murali, R. Deepu, and R. C. Shivamurthy, "ResNet-50 vs VGG-19 vs training from scratch: A comparative analysis of the segmentation and classification of Pneumonia from chest X-ray images," *Global Transitions Proceedings*, vol. 2, no. 2, pp. 375-381, 2021, doi: 10.1016/j.gltp.2021.08.027.

[16] M. O. Khairandish, M. Sharma, V. Jain, J. M. Chatterjee, and N. Z. Jhanjhi, "A Hybrid CNN-SVM threshold segmentation approach for tumor detection and classification of MRI brain images," *IRBM*, vol. 43, no. 4, pp. 290-299, 2022, doi: 10.1016/j.irbm.2021.06.003.

[17] Y. Ding, Q. Yang, Y. Wang, D. Chen, Z. Qin, and J. Zhang, "MallesNet: A multi-object assistance based network for brachial plexus segmentation in ultrasound images," *Medical Image Analysis*, vol. 80, 2022, doi: 10.1016/j.media.2022.102511.

[18] J. S. Bowness *et al.*, "Variability between human experts and artificial intelligence in identification of anatomical structures by ultrasound in regional anaesthesia: a framework for evaluation of assistive artificial intelligence," *British Journal Anaesthesia*, 2024, doi: 10.1016/j.bja.2023.09.023.

[19] Y. Jo *et al*., "Optimal view detection for ultrasound-guided supraclavicular block using deep learning approaches," *Scientific Reports*, vol. 13, 2023, doi: 10.1038/s41598-023-44170-y.

[20] D. Tian *et al.*, "Brachial plexus nerve trunk recognition from ultrasound images: a comparative study of deep learning models," in *IEEE Access*, vol. 10, pp. 82003-82014, 2022, doi: 10.1109/ACCESS.2022.3196356.

[21] L. Cai, Q. Li, J. Zhang, Z. Zhang, R. Yang, and L. Zhang, "Ultrasound image segmentation based on transformer and U-Net with joint loss," *PeerJ Computer Science*, vol. 9, pp. e1638–e1638, Oct. 2023, doi: 10.7717/peerj-cs.1638.

[22] G. Ranganathan, "A study to find facts behind preprocessing on deep learning algorithms," *Journal of Innovative Image Processing*, vol. 3, no. 1, pp. 66-74, 2021, doi: 10.36548/jiip.2021.1.006.

[23] D. Danon, M. Arar, D. Cohen-Or, and A. Shamir, "Image resizing by reconstruction from deep features," *Computational Visual Media*, vol. 7, pp. 453–466, 2021, doi: 10.1007/s41095-021-0216-x.

[24] D. Singh and B. Singh, "Investigating the impact of data normalization on classification performance," *Applied Soft Computing*, vol. 97, pp. 105524, 2020, doi: 10.1016/j.asoc.2019.105524.

[25] F. Ding, Y. Shi, G. Zhu, and Y.-Q. Shi., "Real-time estimation for the parameters of Gaussian filtering via deep learning," *Journal of Real-Time Image Processing*, vol. 17, pp. 17–27, 2020, doi: 10.1007/s11554-019-00907-5.

[26] S. Somasunder and F. Y. Shih, "Land cover image segmentation based on individual class binary masks," *International Journal of Pattern Recognition and Artificial Intelligence*, vol. 35, no. 16, Dec. 2021, doi: 10.1142/s0218001421540343.

[27] B. Koonce, *Convolutional neural networks with swift for tensorflow: image recognition and dataset categorization*, Berkeley, CA: Apress, 2021, doi: 10.1007/978-1-4842-6168-2.

[28] M. A. Chandra and S. S. Bedi, "Survey on support vector machines and their application in image classification," *International Journal of Information Technology*, vol. 13, pp. 1–11, 2021, doi: 10.1007/s41870-017-0080-1.

[29] A. Mohammed and R. Kora, "A comprehensive review on ensemble deep learning: Opportunities and challenges," *Journal of King Saud University-Computer and Information Sciences*, vol. 35, no. 2, pp. 757-774, 2023, doi: 10.1016/j.jksuci.2023.01.014.

BIOGRAPHIES OF AUTHORS

Dr. Sobhana Mummaneni is currently working as an associate professor in the Department of Computer Science and Engineering, V. R. Siddhartha Engineering College, Vijayawada, India. She received Ph.D. degree in Computer Science and Engineering in 2018 from Krishna University. She has 16 years of teaching experience. Her research interests lie in areas such as artificial intelligence, machine learning, data analytics, cyber security, and software engineering. She published 35 papers in national and international journals and published 7 patents. She can be contacted at email: sobhana@vrsiddhartha.ac.in.

Kushal Kumar Chintakayala is a final-year B.Tech. student, specializing in Computer Science and Engineering at V. R. Siddhartha Engineering College, Vijayawada, India. He is passionate about artificial intelligence and machine learning. He is IEEE core member of Computer Society (CS) student chapter. He can be contacted at email: kushalkumarchintakayala12@gmail.com.

Lalith Sai Mukund Yarlagadda is a final-year B.Tech. student, specializing in Computer Science and Engineering at V. R. Siddhartha Engineering College, Vijayawada, India. He is passionate about artificial intelligence and machine learning. He can be contacted at email: mukundyg2002@gmail.com.

Venkata Siva Naga Raju Ala is a final-year B.Tech. student, specializing in Computer Science and Engineering at V. R. Siddhartha Engineering College, Vijayawada, India. He is passionate about artificial intelligence and machine learning. He can be contacted at email: avsnagarajuyadav1999@gmail.com.

Nihitha Vemulapalli is a final-year B.Tech. student specializing in Computer Science and Engineering at V. R. Siddhartha Engineering College, Vijayawada, India. She is passionate about deep learning and has been recognized as a Google Women Engineers Scholar. Additionally, she holds the position of IEEE Chair at the Women in Engineering (WIE) student chapter. She can be contacted at email: nihithavemulapalli@gmail.com.